New tools for studying microglia in the mouse and human CNS

Mariko L. Bennett[a,1], F. Chris Bennett[a,b], Shane A. Liddelow[a,c], Bahareh Ajami[d], Jennifer L. Zamanian[a], Nathaniel B. Fernhoff[e,f,g,h], Sara B. Mulinyawe[a], Christopher J. Bohlen[a], Aykezar Adil[a], Andrew Tucker[a], Irving L. Weissman[e,f,g,h], Edward F. Chang[i], Gordon Li[j], Gerald A. Grant[j], Melanie G. Hayden Gephart[j], and Ben A. Barres[a,1]

[a]Department of Neurobiology, Stanford University School of Medicine, Stanford, CA 94305; [b]Department of Psychiatry and Behavioral Sciences, Stanford University School of Medicine, Stanford, CA 94305; [c]Department of Pharmacology and Therapeutics, University of Melbourne, Melbourne, VIC, Australia, 3010; [d]Department of Neurology, Stanford University School of Medicine, Stanford, CA 94305; [e]Institute for Stem Cell Biology and Regenerative Medicine, Stanford University School of Medicine, Stanford, CA 94305; [f]Ludwig Center for Cancer Stem Cell Research and Medicine, Stanford University School of Medicine, Stanford, CA 94305; [g]Stanford Cancer Institute, Stanford University School of Medicine, Stanford, CA 94305; [h]Department of Pathology, Stanford University School of Medicine, Stanford, CA 94305; [i]University of California, San Francisco Epilepsy Center, University of California, San Francisco, CA 94143; and [j]Department of Neurosurgery, Stanford University School of Medicine, Stanford, CA 94305

Contributed by Ben A. Barres, January 12, 2016 (sent for review November 8, 2015; reviewed by Roman J. Giger and Beth Stevens)

The specific function of microglia, the tissue resident macrophages of the brain and spinal cord, has been difficult to ascertain because of a lack of tools to distinguish microglia from other immune cells, thereby limiting specific immunostaining, purification, and manipulation. Because of their unique developmental origins and predicted functions, the distinction of microglia from other myeloid cells is critically important for understanding brain development and disease; better tools would greatly facilitate studies of microglia function in the developing, adult, and injured CNS. Here, we identify transmembrane protein 119 (Tmem119), a cell-surface protein of unknown function, as a highly expressed microglia-specific marker in both mouse and human. We developed monoclonal antibodies to its intracellular and extracellular domains that enable the immunostaining of microglia in histological sections in healthy and diseased brains, as well as isolation of pure nonactivated microglia by FACS. Using our antibodies, we provide, to our knowledge, the first RNAseq profiles of highly pure mouse microglia during development and after an immune challenge. We used these to demonstrate that mouse microglia mature by the second postnatal week and to predict novel microglial functions. Together, we anticipate these resources will be valuable for the future study and understanding of microglia in health and disease.

microglia | glia | developmental neuroscience | RNAseq | macrophage

Microglia are the resident parenchymal myeloid cells of the CNS, with important roles in development, homeostasis, disease, and injury (1). A major limitation to dissecting microglia-specific contributions to these processes is an inability to distinguish microglia from related cells, such as macrophages. The importance of this distinction is increasingly clear, because microglia not only have unique origins and developmental transcriptional programs, but are self-renewing and function differently than infiltrating macrophages in CNS disease and injury (2–4).

Until recently, methods to distinguish microglia from other CNS cells relied on morphological distinctions (ramified vs. amoeboid), relative marker expression by flow cytometry (the common leukocyte antigen $CD45^{hi/lo}$) (5), or generating bone marrow (BM) chimeras (6, 7). Unfortunately, these approaches have inherent limitations. First, parameters such as morphology or CD45 expression may change with disease or injury. Second, chimeric mouse generation leads to partial chimerism, causes inflammatory damage, and can take many months (8, 9). More recently, tools based on microglial expression of the fractalkine receptor, *Cx3cr1*, overcame some of these limitations. The generation of knockin *Cx3cr1-GFP* (10) and *Cx3cr1-CreERT* (11, 12) mice advanced the specificity and sophistication with which to study microglial function. *Cx3cr1*, however, is also highly expressed by circulating monocytes ($Ly6C^{lo}$) and other tissue resident macrophages (10, 13, 14). In addition, no widely available and well-validated antibodies to known antigens yet exist to specifically and stably identify microglia.

Therefore, we sought a molecular marker that would allow for the identification, isolation, and study of microglia across many applications. Whereas several studies have proposed potential microglia-specific markers (15–17), none have systematically validated these candidates, elucidated whether the markers identified all microglia, or developed microglia-specific antibodies for use by the larger neuroscience community. Here we identify and describe transmembrane protein 119 (Tmem119) as a microglia-specific marker in both mouse and human CNS. We developed rabbit monoclonal antibodies against the intracellular and extracellular domains of mouse Tmem119 for use in immunohistochemical identification and FACS isolation of microglia, respectively. We adapted existing isolation methods to generate what are, to our knowledge, the first ever RNA sequencing profiles of pure, nonactivated microglia during development

Significance

Microglia are the tissue resident macrophages of the brain and spinal cord, implicated in important developmental, homeostatic, and disease processes, although our understanding of their roles is complicated by an inability to distinguish microglia from related cell types. Although they share many features with other macrophages, microglia have distinct developmental origins and functions. Here we validate a stable and robustly expressed microglial marker for both mouse and human, transmembrane protein 119 (Tmem119). We use custom-made antibodies against Tmem119 to perform deep RNA sequencing of developing microglia, and demonstrate that microglia mature by the second postnatal week in mice. The antibodies, cell isolation methods, and RNAseq profiles presented here will greatly facilitate our understanding of microglial function in health and disease.

Author contributions: M.L.B., F.C.B., and B.A.B. designed research; M.L.B., F.C.B., S.A.L., B.A., N.B.F., S.B.M., C.J.B., A.A., and A.T. performed research; M.L.B., J.L.Z., I.L.W., E.F.C., G.L., G.A.G., and M.G.H.G. contributed new reagents/analytic tools; M.L.B., F.C.B., B.A., and B.A.B. analyzed data; M.L.B. and B.A.B. wrote the paper; and I.L.W. performed BMT experiments in his laboratory.

Reviewers: R.J.G., University of Michigan; and B.S., Harvard Medical School Children's Hospital.

The authors declare no conflict of interest.

Freely available online through the PNAS open access option.

Data deposition: The sequence reported in this paper has been deposited in the NCBI BioProject, www.ncbi.nlm.nih.gov/bioproject (accession no. PRJNA307271).

See Commentary on page 3130.

[1]To whom correspondence may be addressed. Email: marikobennett@stanford.edu or barres@stanford.edu.

This article contains supporting information online at www.pnas.org/lookup/suppl/doi:10.1073/pnas.1525528113/-/DCSupplemental.

www.pnas.org/cgi/doi/10.1073/pnas.1525528113

and activated microglia following systemic inflammation. We added these data to a user-friendly website (www.BrainRNAseq.org). For human study, we identified and validated an anti-human TMEM119 rabbit polyclonal antiserum that specifically stains microglia in postmortem and surgical human brain sections. Together, the new microglial tools we developed have the potential to broadly enable studies of microglia function in health and disease.

Results

***Tmem119* mRNA Expression Is Highly Enriched in the CNS and Specific to Most or all Microglia.** To identify a microglia-specific marker, we generated a microglia-enriched gene expression profile of CD45$^+$ immunopanned brain leukocytes from adult mice (18). Comparing these data with our datasets of highly pure CNS cells and profiles of acutely purified immune cells (18–22), we identified seven highly expressed and enriched candidates: *Tmem119*, *Fcrls*, *P2ry12*, *P2ry13*, *Gpr34*, *Gpr84*, *Il1a* (*SI Appendix*, Fig. S1*A*). By in situ hybridization, we found only *Tmem119* was expressed by all parenchymal myeloid cells (Fig. 1 and *SI Appendix*, Fig. S1 *B–F*) but not *C1q*$^+$ choroid plexus or meningeal macrophages (Fig. 1 *D* and *E*), or *Cd163*$^+$ perivascular cells (Fig. 1*F*). *Tmem119*$^+$ cells constituted 93 ± 4% (mean ± SEM) of all *C1q*$^+$ cells in brain sections, whereas all *Tmem119*$^+$ cells were *C1q*$^+$. *Tmem119*$^-$*C1q*$^+$ cells, with rare exception (Fig. 1*C*), were located outside the CNS parenchyma. By quantitative PCR (qPCR), *Tmem119* was highly expressed by CNS CD45$^+$ cells but not BM, spleen, liver, or blood (Fig. 1*G*; blood data not shown for clarity). Taken together, these data demonstrate *Tmem119* is highly expressed by and limited to microglia.

Custom Anti-Tmem119 Monoclonal Antibodies Specifically Identify Microglia. Tmem119 is a type IA single-pass transmembrane protein with a reported role in osteoblast differentiation (23, 24). Because no specific anti-mouse Tmem119 antibodies existed, we made two different monoclonal antibodies (mAbs) against the predicted extracellular (ECD) and intracellular (ICD) domains of mouse Tmem119 (*SI Appendix*, Fig. S2*A*). We stained cryosections from *Cx3cr1*$^{GFP/+}$ × *Tmem119* WT and knockout (KO) mice, as well as WT and KO lacking *Cx3cr1-GFP*. Both mAbs demonstrated robust microglial staining in WT but not KO tissues (Fig. 2 *A* and *G* and *SI Appendix*, Fig. S2*B*). The ICD mAb immunostained the microglial cell surface, revealing many fine processes not apparent by classic markers (Fig. 2 *B* and *C*). Staining was limited to parenchymal Cx3cr1-GFP$^+$ and Iba1$^+$ cells, and absent from meninges or choroid plexus, consistent with *Tmem119* mRNA (Fig. 2 *A–D* and *SI Appendix*, Fig. S2 *C–G*). By flow cytometry, ECD mAbs specifically stained CD45^{lo}CD11b$^+$ cells [presumptive microglia (5)] from healthy adult WT but not KO brains (Figs. 2 *F* and *G* and 3*C*). Tmem119 immunoreactivity (IR) was absent from all explored peripheral sites, including liver, thymus, blood, spleen, and peripheral nerve, even in the context of inflammation or injury (Fig. 2*E* and *SI Appendix*, Fig. S2 *E*, *F*, *H*, and *I*). Together, these results demonstrate that Tmem119 protein expression is highly specific to microglia.

Tmem119 IR Is Developmentally Regulated. We immunostained brain sections from embryonic day (E) 17 to postnatal day (P) 60 mice and found that despite the presence of Iba1$^+$ cells, Tmem119 IR did not appear until P3 to P6 (Fig. 3 *A* and *B* and *SI Appendix*, Fig. S3*A*). By FACS, we found no Tmem119$^+$ cells

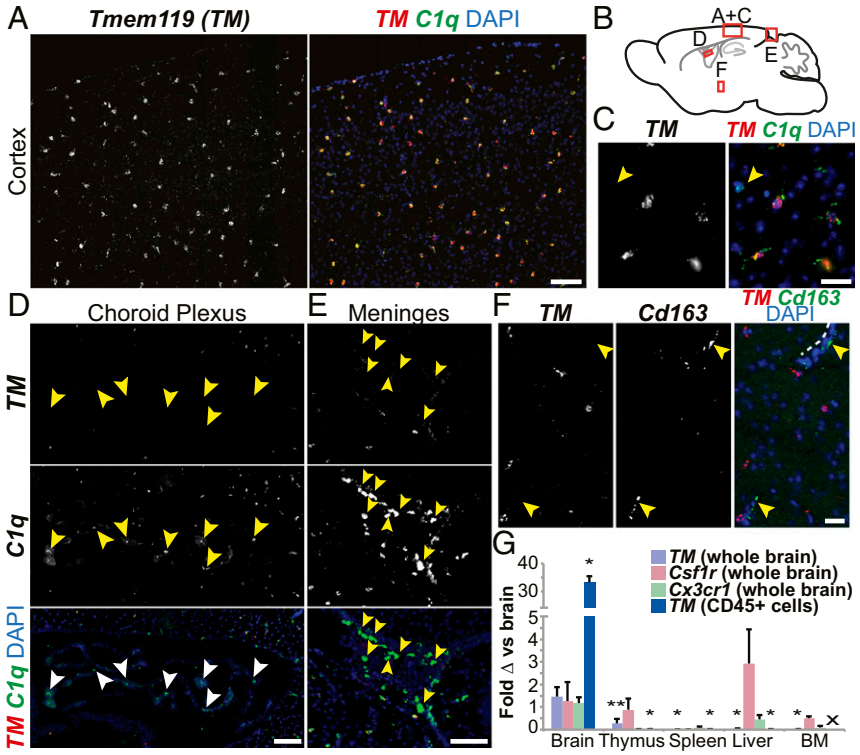

Fig. 1. *Tmem119* is specifically expressed by parenchymal myeloid cells in the CNS. (*A*) In situ hybridization of mouse brain revealed widespread *Tmem119* expression by myeloid (*C1q*$^+$) cells. Composited from two adjacent imaging fields. (*B*) Sagittal brain schematic of panel locations. (*C*) Higher power showing *C1q*$^+$ *Tmem119*$^+$ and a rare parenchymal *C1q*$^+$*Tmem119*$^-$ cell (arrow). *C1q*$^+$ cells in the choroid plexus (*D*) and meninges (*E*) were *Tmem119*$^-$ (arrows). (*F*) *Tmem119* mRNA was not detected in *Cd163*$^+$ perivascular macrophages (arrows; dotted line highlights one vessel). (*G*) qPCR analysis of *Tmem119, Csf1r*, and *Cx3cr1* expression by whole tissues and *Tmem119* by CD45$^+$ cells compared with average expression of each gene in whole brain. Data presented as mean ddCT ± SEM; **P* < 0.01 compared with whole brain *Tmem119*; ***P* < 0.02 by ANOVA with post hoc Tukey HSD for dCT values. *n* = 4–9 except BM, CD45$^+$ liver, CD45$^+$ thymus where *n* = 2. x, no sample for CD45$^+$ BM. (Scale bars: 100 μm in *A*, *D*, and *E*; 40 μm in *C* and *F*.) See also *SI Appendix*, Fig. S1.

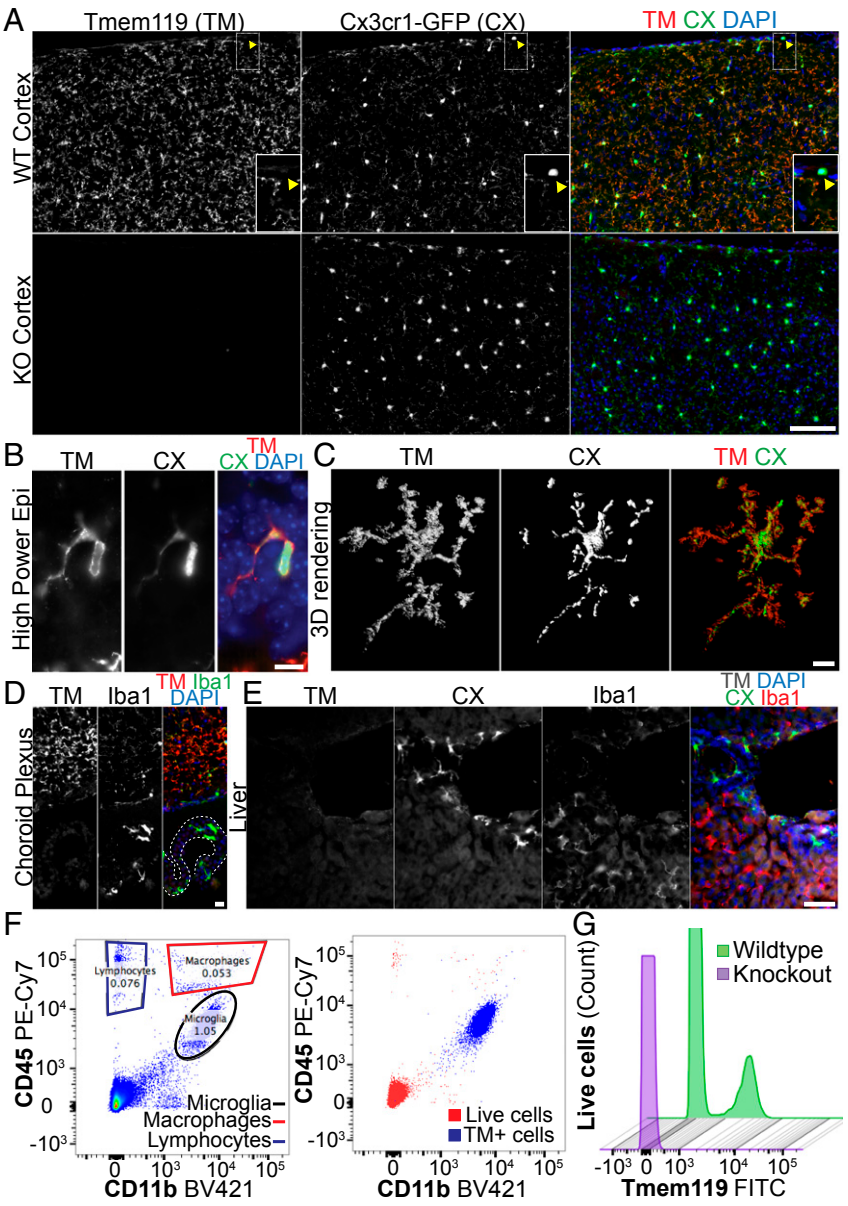

Fig. 2. Monoclonal antibodies reveal microglia-specific Tmem119 IR. (*A*) ICD Tmem119 mAbs stained all Cx3cr1-GFP$^+$ cells except in meninges (arrow and *Inset*) in Tmem119 WT but not KO brain. [Scale bars, 100 μm in *A* (50 μm in *Inset*).] Tmem119 protein localized to microglia cell surface, by epifluorescence (*B*) and confocal microscopy (*C*). (Scale bars, 10 μm in *B*, 7 μm in *C*.) (*D*) Tmem119 IR is limited to myeloid cells in CNS parenchyma and was not detected in choroid plexus (outlined with dotted line) Iba1$^+$ macrophages or liver (*E*). (Scale bars, 50 μm in *D* and *E*.) (*F*) FACS plot schema showing cell populations revealed by CD11b and CD45 expression at P60 (*Left*). Tmem119 (TM$^+$) is restricted to CD45^{lo}CD11b$^+$ microglia (blue cell population, *Right*). (*G*) ECD mAbs are specific, as revealed by staining in WT but not KO brains (*G*). See also *SI Appendix*, Fig. S2.

at E17, whereas by P7 ~25% of CD45^{lo}CD11b$^+$ cells were Tmem119$^+$ (Fig. 3*C*). Between P10 and P14, the number of Tmem119$^+$ microglia increased to adult (P60) levels (P60: 98.1 ± 0.6%, mean ± SEM). We found no mean fluorescence intensity (MFI) difference between young and adult Tmem119$^+$ microglia, suggesting that once IR is detected, Tmem119 protein is expressed at adult levels. Together, these studies demonstrate that by P14 all microglia are Tmem119$^+$.

Tmem119 IR Distinguishes Microglia from Resident and Infiltrating Macrophages After CNS Inflammation and Injury. To assess the utility of Tmem119 as a stable microglia marker, we selected three mouse models of injury and disease: sciatic nerve injury-induced microglial activation, lipopolysaccharide (LPS)-induced systemic inflammation, and optic nerve crush injury. Despite significantly increased Iba1$^+$ IR, we noted no loss of Tmem119$^+$ microglia proximal to the dorsal root entry zone 4 d postsciatic nerve crush injury (*SI Appendix*, Fig. S2 *E* and *F*). For systemic inflammation-induced microglia activation, we injected adult WT mice with PBS or LPS (5 mg/kg, i.p.) (25), and analyzed two to three mice per group at 1 d and 3 d postinjection. As expected, LPS caused increased Iba1 IR and process hypertrophy (Fig. 3*D* and *SI Appendix*, Fig. S3*B*). In addition, all Iba1$^+$ parenchymal cells remained Tmem119$^+$ and staining intensity did not qualitatively decrease at either time point (Fig. 3*D*) (for 3 d). Separately, we quantified Tmem119 IR by FACS 1 d after LPS or PBS. We found no difference in the number or MFI of Tmem119$^+$ cells between groups (Fig. 3*C*) ($P = 0.39$ for MFI, pairwise t test with Bonferroni correction).

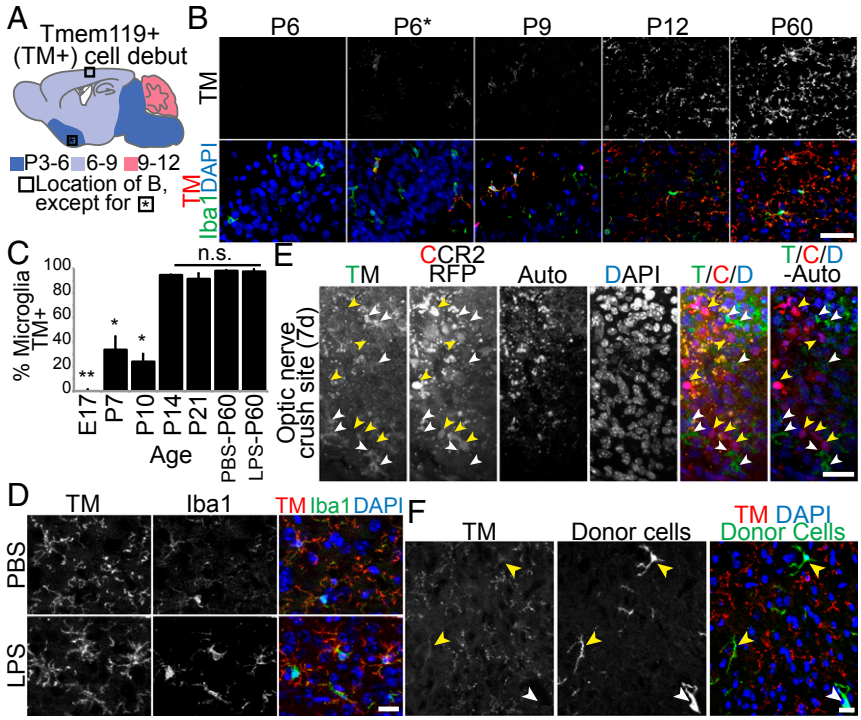

Fig. 3. Tmem119 is a developmentally regulated but stable microglia marker. (*A*) Schematic showing timing of Tmem119 IR in microglia. (Scale bars, 50 μm.) (*B*) Tmem119 and Iba1 IR in brain sections from different ages (maximum intensity projection, MIP). (*C*) Percent Tmem119$^+$ cells by age and post-LPS treatment, using ECD mAb. Bars show mean± SEM *$P < 0.01$ P14–P60; **$P < 0.01$ all ages; n.s., no significant differences by ANOVA with Tukey HSD. $n = 2$ experiments of two animals (P10 and older) or one litter (under P10) for each age/condition, except for P7 ($n = 3$), P21 ($n = 3$), P60 ($n = 8$, 3 PBS injected pooled with naïve). (*D*) Tmem119 and Iba1 IHC 3 d post-PBS or LPS reveals no gross reduction in Tmem119 IR (MIP). (Scale bars, 20 μm.) (*E*) Representative MIP of optic nerve crush site in 120 d CCR2-RFP$^{+/-}$ mouse. Tmem119 (T) IR (white arrows) and CCR2-RFP (C, yellow arrows) detected at the crush site. There are no Tmem119$^+$RFP$^+$ cells. Autofluorescence channel (auto) is digitally subtracted from merge (T/C/D) to differentiate microglia (green) from infiltrating cells (red) in debris-filled crush site. (Scale bars, 25 μm.) (*F*) GFP$^+$ donor BM cells in the CNS 6 mo posttransplant are Tmem119$^-$ in the parenchyma (yellow) and out (white) despite the presence of Tmem119$^+$ microglia. (Scale bars, 20 μm.) See also *SI Appendix*, Fig. S3.

Finally, we investigated whether Tmem119 distinguishes microglia from infiltrating macrophages following optic nerve crush (ONC), a well-established CNS traumatic injury model with monocyte influx and local blood–brain barrier disruption (26, 27). We performed unilateral retro-orbital ONCs in 30 and 120 d CCR2$^{RFP/+}$ mice, which express red fluorescent protein (RFP) only in infiltrating monocytes ($n = 3$, each) (13). We harvested nerves 7 d post-ONC, and processed sections with Tmem119 ICD and anti-Iba1 antibodies. At the crush site, some Iba1$^+$ cells were Tmem119$^-$ (*SI Appendix*, Fig. S3*D*, "x" marks). Iba1$^+$ Tmem119$^-$ cells, with rare exception (*SI Appendix*, Fig. S3*D*, asterisks), were RFP$^+$, indicating these cells infiltrated from the periphery. Although many Iba1$^+$ cells were Tmem119$^+$, these were RFP$^-$, demonstrating that Tmem119 labels resident optic nerve microglia and not infiltrating macrophages. Perhaps most notably, RFP$^+$ cells were never Tmem119$^+$ (Fig. 3*E* and *SI Appendix*, Fig. S3 *D* and *E*), suggesting that even after nerve injury, Tmem119 is a stable marker of resident microglia and not infiltrating macrophages. In summary, in peripheral injury, systemic inflammation (LPS) and traumatic CNS injury (ONC), Tmem119 specifically labeled only resident microglia, allowing for the visualization of microglia after inflammation and injury and providing a clear distinction between resident and infiltrating myeloid cells.

BM-Derived Cells in the Adult CNS Do Not Express Tmem119. Microglia normally arise from yolk-sac progenitors (3). After some forms of brain injury, BM macrophages can take residence in the brain (8). Because of the lack of markers to distinguish microglia from macrophages, it was unclear if engrafted BM macrophages transform into microglia. We performed a modified BM transplant conditioning regimen with GFP$^+$ donor BM to bolster CNS engraftment (*SI Appendix, Experimental Procedures*) We euthanized mice 3 and 6 mo ($n = 2$ and 3 animals, respectively, for conditioned; $n = 1$ and 1 for naïve) after transplant and examined if engrafted BM cells in the brain were Tmem119$^+$. At both time points, we observed GFP$^+$ cells along the meninges, in blood vessels, and in parenchyma of conditioned but not unconditioned mice. We noted more GFP$^+$ cells with complex, ramified morphology in the CNS parenchyma at 6 vs. 3 mo, although regionally, engraftment rates were never >15% of Iba1$^+$ cells. All GFP$^+$ cells were Iba1$^+$ (*SI Appendix*, Fig. S3*F*). At both time points, however, we observed no or extremely low Tmem119 IR in GFP$^+$ cells, despite robust Tmem119 IR of GFP$^-$Iba1$^+$ cells (Fig. 3*F* and *SI Appendix*, Fig. S3 *F* and *G*). These data indicate that the adult CNS does not induce Tmem119 IR in BM cells and that engrafted BM myeloid cells retain their nonmicroglial identity, even after 6 mo in the CNS.

Elucidation of Developing, Adult, and Activated Microglial Transcriptomes from Tmem119-Purified Microglia. Given the specificity and developmental regulation of Tmem119 in microglia, we wanted to generate a highly pure RNAseq profiling resource to better understand microglial development, maturation, and activation. We modified existing microglia isolation protocols (28, 29) to formulate a method that resulted in the most nonactivated and pure microglia profiles possible (Fig. 4*A*). We dounce-homogenized brains, performed MACS-based myelin depletion, and sorted cells with Tmem119 ECD mAbs. We double-sorted to obtain >99% purity as assessed by flow cytometry and RNAseq expression of cell-type–specific markers

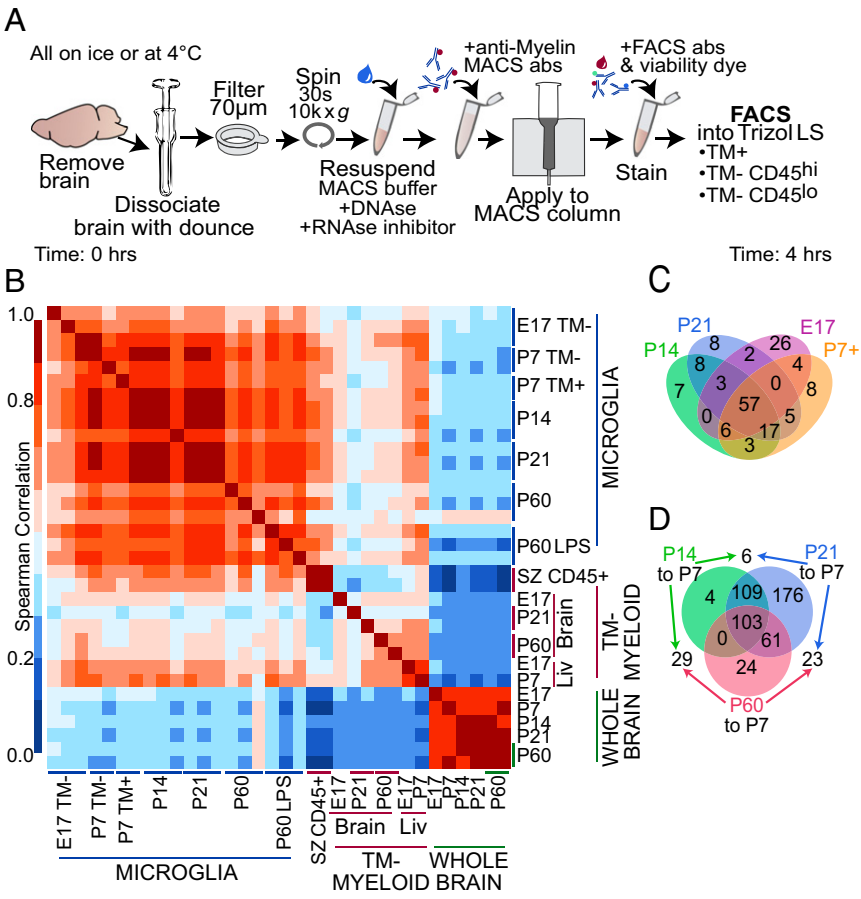

Fig. 4. Isolation and RNAseq profiling of microglia using Tmem119 IR. (*A*) Schematic showing streamlined microglia isolation procedure for minimizing baseline microglia reactivity and death. Abbreviations: abs, antibodies; CV, column volumes; TM, Tmem119. (*B*) Heatmap of Spearman correlation between individual microglia, myeloid, and whole-tissue RNAseq replicates for genes expressed FPKM > 5. (*C*) Four-way diagram demonstrating top 100 expressed genes by microglia (Tmem119$^+$ except for E17) at each age. (*D*) Venn diagram showing number of differentially expressed genes between P7 Tmem119$^+$ and mature microglia (P14, P21, P60). Black numbers outside diagram represent the few differentially expressed genes between these time points. Diagrams adapted from jVenn (58). See also *SI Appendix*, Fig. S4 and Dataset S1.

(Fig. 2*F* and *SI Appendix*, Fig. S4*A*). We generated two to three replicates for the following microglia samples: E17 (CD45^{lo} CD11b$^+$Tmem119$^-$), P7$^-$ (CD45^{lo}CD11b$^+$Tmem119$^-$), P7$^+$ (Tmem119$^+$), P14 (Tmem119$^+$), P21 (Tmem119$^+$), and P60 (Tmem119$^+$). We also collected Tmem119$^+$ cells from P60 mice 24 h after 5 mg/kg, i.p. LPS (n = 3). We generated two replicates each of P60 and P21 nonmicroglia myeloid cells (CD45^{hi}CD11b$^+$Tmem119$^-$), one sample each for myeloid cells from E17 brain, E17 liver, P7 liver (hereafter "myeloid cells" for clarity) and whole brain for each age (n = 1 for E17–P21, n = 2 for P60) (Fig. 4*B*). We generated cDNA libraries and performed RNAsEq. (30), obtaining 27.6 ± 7.1 million paired-end 75-bp reads per replicate, and mapped and analyzed these data using the Tuxedo suite of tools (31) and edgeR (32) (see *SI Appendix* for details).

The full Cufflinks-generated fragments per kilobase per million (FPKM) dataset and edgeR differential expression analyses are available as Dataset S1, and on a custom website to view in comparison with our laboratory's other CNS cell type datasets: www.BrainRNAseq.org. Raw sequencing files are available from National Center for Biotechnology Information (NCBI) BioProject (accession no. PRJNA30727).

RNAseq Profiles Quality and Purity: Lower Expression of Activation Marker Genes. We assessed the quality and purity of our RNAseq profiles by mapping quality and the expression of cell-type–specific and activation-associated genes. We mapped >58% of reads for all, and >70% of reads for most (n = 30) samples. As expected, myeloid-specific genes were highly enriched, with very low expression of other cell-type–specific genes (*SI Appendix*, Fig. S4*A*). These results reflect purity and that Tmem119 IR is sufficient to isolate microglia by P14. We calculated percentile ranks for several canonical activation genes for our naïve and LPS-stimulated samples, as well as five published datasets (15, 17, 30, 33, 34); these datasets were generated using CD45 or Cx3cr1 rather than a specific microglia marker, such as Tmem119, and used enzymatic digestion or Percoll for dissociation and myelin depletion. Compared with published profiles, canonical activation marker expression (*Tnf*, *Il1b*, *Nfkb2*) was significantly reduced in our naïve microglia, providing evidence that our procedure limits microglial activation (*SI Appendix*, Fig. S4*B*).

Microglial Maturation Occurs by P14 and Correlates with Tmem119 Gene Expression. The precise onset of Tmem119 IR made us wonder about differences between microglia before and after P14. First, we compared microglia, myeloid cell, and whole-brain RNA expression profiles and found that microglia were highly similar throughout development, with more variability between biological replicates at P60 (Fig. 4*B*). We clustered the averaged samples (35) and identified two distinct branches for microglia and CNS myeloid cells (*SI Appendix*, Fig. S4 *C* and *D*), highlighting differences between these cell types.

Microglia clustered by age with relatively small heights between branches, indicative of their highly correlated gene expression (*SI Appendix*, Fig. S4*C*). Indeed, 57 of the 100 most highly expressed genes were shared from E17–P21 (Fig. 4*C*). These include known microglia-enriched genes, such as *Cx3cr1*, *P2ry12*, *Csf1r*, and *Fcrls.* After P14, few genes were differentially expressed (Fig. 4*D*), whereas most differences between P14, P21, and P60, each compared with P7 Tmem119^{+} microglia, were shared. In contrast to younger ages, most differentially expressed genes at and after P14 were lowly expressed at all ages (FPKM < 10) or a consequence of low-level synaptic contamination in some P60 replicates (*Gad2*, *Snap25*, *Oprm1*, *Vsnl1*, *Pclo*, *Bdnf*), evidenced by RNAseq reads in some but not all replicates. Given the small number of gene expression differences between microglia over P14, we concluded that microglia mature by P14.

Despite a lack of Tmem119 IR in 100% of E17 and 75% of P7 microglia (Fig. 3*C*), our RNAseq profiles revealed robust *Tmem119* expression at these ages, with an FPKM of 168 and 390, respectively (Fig. 5*A* and Dataset S1). By P14, *Tmem119* expression increased 6.8-fold to adult levels. Surprisingly, there was no difference in *Tmem119* expression between P7^{+} and P7^{-} microglia, possibly suggesting an uncoupling of transcription and translation and that *Tmem119*-driven gene expression could be a robust microglial marker before IR.

With Maturity, Microglia-Enriched Gene Expression Increases, While Proliferation Decreases. Although microglial gene expression is highly correlated throughout development, we were interested in genetic changes that may underlie development-specific functions. First, we examined the top up- and down-regulated genes between E17 and "adult" (P21 and P60) microglia (*SI Appendix*, Table S1). A cassette of microglia-enriched genes were up-regulated, including *Tmem119*, *P2ry13*, and *Olfml3.* We generated a list of genes expressed by Tmem119^{+} microglia versus Tmem119^{-} myeloid cells and found that 37 of 100 top microglia-enriched genes are up-regulated from E17 to adulthood (Fig. 5*A* and *SI Appendix*, Table S2). We validated a selection of these genes by microfluidics-based qPCR and in situ (*SI Appendix*, Fig. S5 *E*, *G*, and *H*). Although not all microglia-enriched genes demonstrated this trend, many reached their mature levels by P14. Given our interest in *Tmem119* expression patterns and microglial maturity, we performed unsupervised hierarchical clustering of our microglial and published RNAseq datasets (30) to find other similarly behaved genes (*SI Appendix*, Table S3 and Dataset S1, "clusterID" column). The gene cluster of *Tmem119* not only contained many microglia-enriched genes, but a number of genes associated with leukocyte development, differentiation, and homeostasis: *Blnk*, *Inpp5d*, *Rgs10*, *Mef2c*, *Cysltr1*, *Orai1*, *Ifngr1*, *Pnp*, *Casp8*, and *Tgfbr1* (*SI Appendix*, Table S3, Ingenuity Pathway Analysis).

Cell cycle-associated genes were among the top down-regulated genes we identified during microglia development (Fig. 5*B* and *SI Appendix*, Fig. S5*A* and Table S1). Given the inverse correlation between cell-cycle gene expression and the postnatal appearance of Tmem119 IR, we asked if Tmem119 IR, as a proxy for microglial maturity, corresponded with the end of microglia proliferation. We stained brain cryosections from E14, E17, P6, P12, and P60 mice (n = 2 each) with anti-Ki67, Tmem119 ICD, and Iba1 antibodies (Fig. 5*C*). We quantified the relative percentages of proliferating (Ki67^{+}) and nonproliferating (Ki67^{-}) Iba1^{+} cells and their Tmem119 IR (Fig. 5*D*). Proliferating Iba1^{+} cells were seen at E14 and E17, but only rarely >P6. No proliferating Tmem119^{+}Iba1^{+} cells were detected at any age, and <5% of Iba1^{+} cells at P6 were Tmem119^{+}. By P12, Tmem119^{-}Iba1^{+} cells were still present, despite the end of microglial proliferation more than a week earlier. Together, these data show that although immature microglia before P6 are more proliferative in vivo, Tmem119 IR is not directly related to the termination of proliferation.

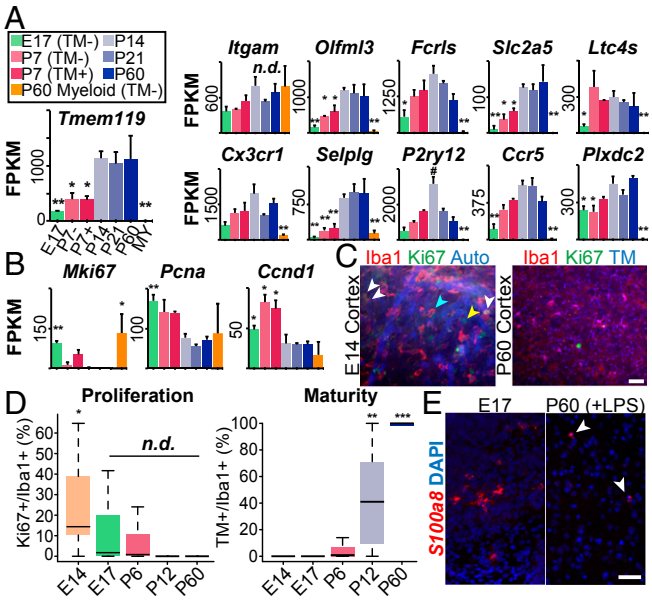

Fig. 5. Developmental changes in microglial gene expression. Bar plots of RNAseq data showing FPKM expression of selected microglia-enriched (*A*) and proliferation marker genes (*B*) by developing microglia and myeloid cells. Error bars depict mean ± SEM $^{**}P < 0.01$, $^{*}P < 0.05$ for values compared with each P60, P21, and P14 microglia; $^{\#}P < 0.01$ compared with P60. (*C*) Representative Ki67, Tmem119, and Iba1 epifluorescence image quantified in *D*, showing Iba1^{+}Ki67^{+} (white arrowheads), Iba1^{+}only (cyan), and Ki67^{+}only (yellow) cells. Auto: autofluorescence. (*D*) Box-and-whisker plots depicting percentage of Iba1^{+} cells that were Ki67^{+} (*Left*) and Tmem119^{+} (*Right*). n.d., no difference; $^{*}P < 0.01$ compared each with P6, P12, and P60; $^{**}P < 0.01$ compared with P6; $^{***}P < 0.01$ compared with P6 and P12; n = 2 mice each, quantified four to eight fields from two to three sections. Box/whiskers represent standard values. All P values calculated by one-way ANOVA with Tukey HSD and verified by pairwise t test with Bonferroni correction. (*E*) In situ of *S100a8* at E17 and P60, the latter 24 h after LPS injection, revealing bright, *S100a8*-expressing cells not detected in naïve P60 brain (not shown). (Scale bars, 50 μm.) See also *SI Appendix*, Fig. S5 and Tables S2–S8.

Other Analyses: Microglial Activation, Ligands/Receptors/Transcription Factors, and Platelets. Given our low baseline activation of Tmem119-sorted microglia, we wanted to determine the transcriptome of "classically" activated microglia. As discussed, we also sequenced microglia 24 h post-LPS injection. LPS-treated microglia up-regulated the expression of many myeloid cell inflammation-associated transcripts, including *Lcn2*, *Ccl3*, *Cxcl10*, *Ccl5*, *Il1b*, *Tnf*, and *Tlr2* (*SI Appendix*, Table S4). Several microglia-enriched genes were also down-regulated, including *P2ry12* and *Tmem119*, *Fcrls*, *Olfml3*, *Ltc4s*, and *Adora3* (*SI Appendix*, Table S4 and Dataset S1). We validated several of these by qPCR (*SI Appendix*, Fig. S5*F*). Pathway analysis (Qiagen) revealed increased Toll-like receptor (TLR), vitamin D3-receptor/RXR activation, and acute phase response signaling pathways (*SI Appendix*, Fig. S5*B*) between naïve and LPS-treated microglia. Together, these results suggest that microglia respond to peripheral LPS with a classic-type activation profile and that some microglia-enriched transcripts are down-regulated. The notion that expression of microglial markers is sensitive to activation state is intriguing, as is the stability of Tmem119 IR despite decreased mRNA expression (Fig. 3 *C* and *D*).

Among the top genes expressed by E17 versus adult microglia are several classes of genes associated with myeloid cell activation. Given the attributed functions of these enriched genes, and published hypotheses that young microglia, which are highly phagocytic and less ramified, might be activated (36), we compared our young microglia with LPS-treated microglia. Several

top LPS-induced genes were expressed more highly by E17 than adult microglia (Fig. 5*E* for *S100a8* in situ, and *SI Appendix*, Table S4, bold genes). Despite these similarities, we found more differences than similarities between young and activated microglia (*SI Appendix*, Fig. S5*D*).

We also generated a list of known transcription factors, ligands, and receptors enriched in microglia over CNS myeloid cells, whole brain, and other CNS cell types (*SI Appendix*, Table S5). We curated a list of disease-associated genes (*SI Appendix*, Table S6), transcription factors (*SI Appendix*, Table S7), and platelet-enriched genes highly enriched in microglia (*SI Appendix*, Table S8).

Tmem119 Is also a Specific Marker of Human Microglia. Tmem119 is highly conserved, with 73% sequence homology between mouse and humans. To test the specificity of *TMEM119* expression to human microglia, we quickly harvested CD11B$^+$ cells sorted from intraoperatively obtained, normal-appearing temporal lobe cortical tissue (n = 2; 47 and 8 y), and compared *TMEM119* expression by qPCR with unpurified whole brain (n = 2; pooled adult and 45 y) and peripheral blood leukocytes (n = 2; pooled adult and 66 y) (Fig. 6*A*). We also examined the expression of *CX3CR1* and *CD11B* as positive controls. *TMEM119* expression was highly enriched in CD11b$^+$ cells over whole brain, and barely detectable in peripheral blood leukocytes, despite the presence of *CD11B*. We tested several commercially available anti-TMEM119 antibodies on human surgical brain specimens, identifying a rabbit polyclonal anti-human TMEM119 antibody that stained only CNS parenchymal Iba1$^+$ cells (Fig. 6*B*). TMEM119 antisera stained the plasma membrane of most or all parenchymal Iba1$^+$ cells (microglia) in both gray and surrounding white matter from rapidly fixed surgical tissue from multiple patients (n = 4; ages 8, 47, 51, and 71 y). Despite the sequence homology between mouse and human Tmem119, neither the anti-mouse mAbs nor the anti-human polyclonal antisera worked to stain microglia in human or mouse, respectively. Together, these findings demonstrate that Tmem119 is a microglia marker in human CNS tissue as well as in mouse.

Discussion

Tmem119 Is a Specific and Stable Marker of Microglia in Mouse and Human. In this study, we show that Tmem119, a transmembrane protein of unknown function, is a developmentally regulated and highly specific cell-surface marker of most or all microglia that is not expressed by macrophages or other immune or neural cell types. *Tmem119* expression is abundant in prenatal microglia but IR—detected by two custom monoclonal antibodies—correlates with microglial maturity postnatally. These antibodies (Abcam, catalog nos. ab209064 ICD and ab210405 ECD) stably identify microglia, even after injury and inflammation. In addition, we optimized a method for isolating pure, nonactivated microglia using these antibodies. Tmem119 is also a specific marker of human microglia, for which we identified a polyclonal antibody to stain microglia in human brain cryosections (Abcam, catalog no. ab185333). These antibodies provide a powerful tool for specifically identifying microglia in future studies of the roles of microglia in CNS health and disease. In addition, the ECD mAb to mouse Tmem119 enabled us to develop a FACS method to prospectively isolate highly pure microglial cells. These purified cells can be used for biochemical studies, culture, or RNA isolation for gene expression studies.

RNAseq Profiles of Developing Microglia Reveal That Microglia Mature by P14. Using the Tmem119 mAbs we generated here, we produced, to our knowledge, the first highly pure RNAseq profiles of microglia during development. These data are publicly accessible through www.BrainRNAseq.org. This resource will help foster the formation and testing of new hypotheses about microglial development and function. Using these profiles, we made several novel observations about microglial function during development. First, mouse microglia mature in vivo by P14, with few genetic differences between P14, P21, and P60 microglia. Both Tmem119 IR and microglia-enriched gene expression increase throughout development until P14, when they stabilize. These observations raise an important question for future studies: what signals induce microglial maturation? For example, is microglia maturation induced at P14 by a systemic endocrine signal or does CNS brain maturation induce a signal that acts on microglia?

In addition, microglial proliferation ceases days before maturation at P14. What is the relationship of microglial proliferation to maturity, and then to activation? In peripheral nerve injury, such as that in *SI Appendix*, Fig. S2*F*, microglia proliferate in the spinal cord by 2 d postinjury (37–39). We showed that all Iba1$^+$ cells in spinal cord are Tmem119$^+$ even after injury, suggesting that mature, Tmem119$^+$ microglia are able to proliferate after injury. Are the signals regulating developmental and activation-induced microglial proliferation different? What are the disease-related implications of these different signals?

Microglia Transcriptome Suggests Potential Novel Functions for Microglia in Health and Disease. Our microglia RNAseq transcriptomes revealed the expression of ligands, receptors, and disease-associated genes, which strongly suggest new microglial functions in development and disease. In addition to known chemokines, Toll-like signaling, and phagocytosis mediators,

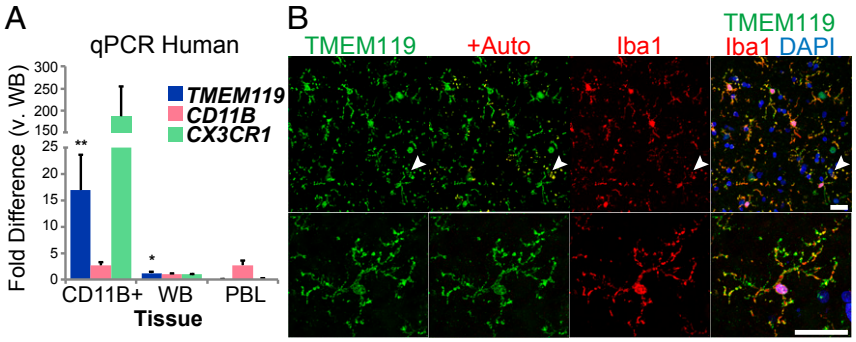

Fig. 6. Tmem119 is also highly enriched in and specific to human microglia. (*A*) Relative expression of *TMEM119*, *CD11B*, and *CX3CR1* mRNA in human peripheral blood leukocytes (PBL), whole brain (WB), and CD11B$^+$ brain cells *P < 0.01 by ANOVA with Tukey HSD. Error bars show SEM, for n = 2 independent samples per tissue type. (*B*) Representative confocal images of 51-y-old normal appearing cortical tissue showing localization of TMEM119 (green) to highly ramified, Iba1$^+$ cells (red) at low (*Upper*) and high (*Lower*) magnification. Autofluorescence channel (red) overlays green to highlight nonspecific fluorescence from lipofuscin (arrows), which are absent in *Lower* because of Sudan Black treatment. (Scale bars, 30 μm.)

microglia also express many other genes of interest. For example, microglia express *Pdgfb*, which is involved in normal pericyte-mediated microvascular development (40, 41), as highly as endothelial cells. Indeed, it is expressed by microglia throughout development, suggesting a potential novel role for early-arriving microglia in vascular development. In addition, microglia express *Pdgfa* (42), a mitogen that is critical for oligodendrocyte generation, and highly express *Sparc*, which helps regulate synapse formation (43).

We found that microglia express high levels of *Hprt*, a purine salvage pathway gene that is deficient in Lesch-Nyhan syndrome (*SI Appendix*, Table S5) (44). This disease is characterized by hyperuricemia and progressive neurological symptoms, which include self-mutilation and intellectual disability. Another highly expressed gene is *Comt*, the enzyme responsible for the degradation of catecholamines (dopamine, epinephrine, norepinephrine), which is targeted by inhibitors to increase the efficacy of L-DOPA treatments for Parkinson disease patients, and is strongly associated with schizophrenia (45). Several metabolic and storage disorders, such as Tay-Sachs, Hurler, neuronal ceroid lipofuscinosis, and peroxisomal biogenesis disorders, also have causal genes that are highly expressed by microglia, suggesting underlying pathology that might begin with microglial dysfunction (*SI Appendix*, Table S5). Microglia, as previously reported, also highly express *Trem2*, rare variants of which are associated with Alzheimer disease (46, 47). Understanding more about the normal role of these microglial genes has great potential to contribute to our understanding of the pathophysiology of neurological disorders.

Our RNAseq profiles also revealed expression differences in immune effector genes (*SI Appendix*, Fig. S5*C* and Table S2), which could have important implications for divergent homeostatic and injury-related responses of microglia and myeloid cells. Given the recently identified novel role for the complement cascade and microglia in synaptic phagocytosis in normal development and disease (48), we compared expression of relevant genes in microglia and CNS macrophages. The upstream classic complement cascade proteins opsonize synapses for microglial engulfment of synapses. Compared with macrophages and other myeloid cells, microglia express many-fold higher levels of *C1qa*, *-b*, and *-c*, as well as the chemotactic receptor *C3ar1* (*SI Appendix*, Table S2 and Dataset S1). Microglia also express significantly higher levels of opsonins (*Pros1*, *Gas6*) that promote synaptic phagocytosis by astrocytes (49). These differences suggest that microglia may be specialized for their role in synapse pruning in health and disease.

Could microglia contribute to hemostatic functions in the CNS? Pathway analysis revealed that both the extrinsic and intrinsic coagulation pathways are down-regulated in microglia versus myeloid cells (*SI Appendix*, Fig. S5*C*), based in part on the limited expression of clotting factors normally produced by the liver (*F5*, *F10*), and the abundance of anticoagulation genes, such as protein S (*Pros1*) and tissue factor pathway inhibitor (*Tfpi*) in microglia (*SI Appendix*, Table S8). We also noted an abundance of platelet-enriched genes (50) that are enriched in microglia versus macrophages, including *P2ry12*, *Pros1*, *Tfpi*, *Gp9* (glycoprotein 9, one component of the von Willebrand factor receptor), *Itga6* (a laminin receptor on platelets) (51), and *Ptgs1* [which in platelets, with *Tbxas1*—also highly expressed by microglia—produces Txa2 to induce platelet aggregation (52, 53)] (*SI Appendix*, Table S8, and Dataset S1). Previously, transcranial two-photon imaging studies of *Cx3cr1*$^{GFP/+}$ mice revealed rapid microglia process chemotaxis toward sites of laser-induced cerebral vessel injury, quickly patching microvessel leaks and apparently "shielding" the brain from hemorrhage (54). Such injury-induced responses are mediated by P2Y receptors, and in particular *P2ry12* (55, 56). Indeed, a recently published study suggests that *P2ry12*-mediated chemotaxis directly influences CNS hemostasis, a finding of great interest in the context of our transcriptomic data, and one that could inform future therapeutic interventions (57).

Tmem119-Based Tools for Future Microglia Study. The tools generated in this study are now available to the research community. The monoclonal anti-mouse Tmem119 antibodies are available from Abcam (catalog nos. ab209064 and ab210405). The RNAseq dataset, as discussed, is available at www.BrainRNAseq.org. Protocols are available in *SI Appendix*, as well as upon request. In addition to the few hypotheses suggested here about microglia-specific function, we anticipate these new antibody and RNAseq profile resources will facilitate the identification and testing of many more.

Additionally, the identification of Tmem119 as a microglia-specific marker can be used to develop further essential tools, such as a Tmem119 promoter-driven Cre recombinase mouse for highly specific gene targeting of microglia throughout development, given the early expression of *Tmem119* transcript, and the first highly pure human microglia transcriptome. Furthermore, the identification of Tmem119 IR as a marker of mature microglia suggests that there might exist other proteins, which mark immature microglia, the pursuit of which is enabled by the new tools generated in the present study.

Finally, what does Tmem119 do? It is one of the most highly expressed microglia-specific genes and is expressed on the cell surface. What does its regulation during development mean for microglial function? What happens when microglia do or do not express Tmem119? We hope that these resources will allow many new studies of microglial function in health and disease.

Experimental Procedures

Human Tissue. Human brain tissue was obtained with informed consent under approved protocols of the Stanford University Institutional Review Board, intraoperatively from neurosurgical cases in collaboration with the Stanford Tissue Bank or University of California, San Francisco, Department of Neurosurgery.

Vertebrate Animals. All procedures involving mice were conducted in conformation with Stanford University guidelines that are in compliance with national and state laws and policies.

Most procedures are described in the text. For detailed cell purification, RNA in situ, mAb generation and use, injury and transplantation models, RNA isolation, sequencing and analysis methods, see *SI Appendix, Experimental Procedures*.

ACKNOWLEDGMENTS. We thank members of the B.A.B. laboratory, particularly S. Sloan, L. Clarke, and Y. Zhang for help with RNAseq library preparation and consultation; A. Ring for critical insights in producing the Tmem119 immunogens; R. Sinha for cDNA for pilot studies; R. Kita for website design; C. Shatz, T. Wyss-Coray, and M. Porteus; and E. Hotz for developmental neuroscience expertise. We thank the Stanford Neuroscience Microscopy Service, especially A. Olson, supported by National Institutes of Health (NIH) Grant NS069375; and the entire staff at the Stanford Shared FACS Facility, supported by NIH S10 Shared Instrument Grant and S10RR025518-01. This work was funded by the NIH Grants R21HD075359, R47DA15043 (to B.A.B.); National Research Service Award predoctoral Fellowship F31 NS078813 (to M.L.B.); National Research Service Award postdoctoral Fellowship F32HL115963-02 (to N.B.F.); T32 training Grants 5T32MH019938-22 (to F.C.B.) and 5K08NS075144-05 (to G.A.G.); the Australian National Health and Medical Research Council postdoctoral Fellowship GNT1052961 (to S.A.L.); a Canadian Institutes of Health Research Fellowship (to B.A.); the Myelin Repair Foundation (B.A.B.); and the Dr. Miriam and Sheldon G. Adelson Medical Research Foundation, JPB Foundation, and Vincent and Stella Coates.

1. Aguzzi A, Barres BA, Bennett ML (2013) Microglia: Scapegoat, saboteur, or something else? *Science* 339(6116):156–161.
2. Alliot F, Godin I, Pessac B (1999) Microglia derive from progenitors, originating from the yolk sac, and which proliferate in the brain. *Brain Res Dev Brain Res* 117(2):145–152.
3. Ginhoux F, et al. (2010) Fate mapping analysis reveals that adult microglia derive from primitive macrophages. *Science* 330(6005):841–845.
4. Sheng J, Ruedl C, Karjalainen K (2015) Most tissue-resident macrophages except microglia are derived from fetal hematopoietic stem cells. *Immunity* 43(2):382–393.

5. Ford AL, Goodsall AL, Hickey WF, Sedgwick JD (1995) Normal adult ramified microglia separated from other central nervous system macrophages by flow cytometric sorting. Phenotypic differences defined and direct ex vivo antigen presentation to myelin basic protein-reactive CD4+ T cells compared. *J Immunol* 154(9):4309–4321.
6. Lassmann H, Schmied M, Vass K, Hickey WF (1993) Bone marrow derived elements and resident microglia in brain inflammation. *Glia* 7(1):19–24.
7. Ajami B, Bennett JL, Krieger C, Tetzlaff W, Rossi FMV (2007) Local self-renewal can sustain CNS microglia maintenance and function throughout adult life. *Nat Neurosci* 10(12):1538–1543.
8. Mildner A, et al. (2007) Microglia in the adult brain arise from Ly-6ChiCCR2+ monocytes only under defined host conditions. *Nat Neurosci* 10(12):1544–1553.
9. Capotondo A, et al. (2012) Brain conditioning is instrumental for successful microglia reconstitution following hematopoietic stem cell transplantation. *Proc Natl Acad Sci USA* 109(37):15018–15023.
10. Jung S, et al. (2000) Analysis of fractalkine receptor CX(3)CR1 function by targeted deletion and green fluorescent protein reporter gene insertion. *Mol Cell Biol* 20(11): 4106–4114.
11. Yona S, et al. (2013) Fate mapping reveals origins and dynamics of monocytes and tissue macrophages under homeostasis. *Immunity* 38(1):79–91.
12. Parkhurst CN, et al. (2013) Microglia promote learning-dependent synapse formation through brain-derived neurotrophic factor. *Cell* 155(7):1596–1609.
13. Saederup N, et al. (2010) Selective chemokine receptor usage by central nervous system myeloid cells in CCR2-red fluorescent protein knock-in mice. *PLoS One* 5(10): e13693.
14. Gautier EL, et al.; Immunological Genome Consortium (2012) Gene-expression profiles and transcriptional regulatory pathways that underlie the identity and diversity of mouse tissue macrophages. *Nat Immunol* 13(11):1118–1128.
15. Chiu IM, et al. (2013) A neurodegeneration-specific gene-expression signature of acutely isolated microglia from an amyotrophic lateral sclerosis mouse model. *Cell Reports* 4(2):385–401.
16. Butovsky O, et al. (2014) Identification of a unique TGF-β-dependent molecular and functional signature in microglia. *Nat Neurosci* 17(1):131–143.
17. Gosselin D, et al. (2014) Environment drives selection and function of enhancers controlling tissue-specific macrophage identities. *Cell* 159(6):1327–1340.
18. Zamanian JL, et al. (2012) Genomic analysis of reactive astrogliosis. *J Neurosci* 32(18): 6391–6410.
19. Edgar R, Domrachev M, Lash AE (2002) Gene Expression Omnibus: NCBI gene expression and hybridization array data repository. *Nucleic Acids Res* 30(1):207–210.
20. Hieronymus T, et al. (2005) Progressive and controlled development of mouse dendritic cells from Flt3+CD11b+ progenitors in vitro. *J Immunol* 174(5):2552–2562.
21. Martinez FO, Gordon S, Locati M, Mantovani A (2006) Transcriptional profiling of the human monocyte-to-macrophage differentiation and polarization: new molecules and patterns of gene expression. *J Immunol* 177(10):7303–7311.
22. Sung L-Y, et al. (2006) Differentiated cells are more efficient than adult stem cells for cloning by somatic cell nuclear transfer. *Nat Genet* 38(11):1323–1328.
23. Hisa I, et al. (2011) Parathyroid hormone-responsive Smad3-related factor, Tmem119, promotes osteoblast differentiation and interacts with the bone morphogenetic protein-Runx2 pathway. *J Biol Chem* 286(11):9787–9796.
24. Tanaka K, et al. (2012) Interaction of Tmem119 and the bone morphogenetic protein pathway in the commitment of myoblastic into osteoblastic cells. *Bone* 51(1):158–167.
25. Chen Z, et al. (2012) Lipopolysaccharide-induced microglial activation and neuroprotection against experimental brain injury is independent of hematogenous TLR4. *J Neurosci* 32(34):11706–11715.
26. Perry VH, Brown MC, Gordon S (1987) The macrophage response to central and peripheral nerve injury. A possible role for macrophages in regeneration. *J Exp Med* 165(4):1218–1223.
27. Frank M, Wolburg H (1996) Cellular reactions at the lesion site after crushing of the rat optic nerve. *Glia* 16(3):227–240.
28. Pino PA, Cardona AE (2011) Isolation of brain and spinal cord mononuclear cells using percoll gradients. *J Vis Exp* (48):2348.
29. Nikodemova M, Watters JJ (2012) Efficient isolation of live microglia with preserved phenotypes from adult mouse brain. *J Neuroinflammation* 9(1):147.
30. Zhang Y, et al. (2014) An RNA-sequencing transcriptome and splicing database of glia, neurons, and vascular cells of the cerebral cortex. *J Neurosci* 34(36):11929–11947.
31. Trapnell C, et al. (2012) Differential gene and transcript expression analysis of RNA-seq experiments with TopHat and Cufflinks. *Nat Protoc* 7(3):562–578.
32. Robinson MD, McCarthy DJ, Smyth GK (2010) edgeR: A Bioconductor package for differential expression analysis of digital gene expression data. *Bioinformatics* 26(1): 139–140.
33. Lavin Y, et al. (2014) Tissue-resident macrophage enhancer landscapes are shaped by the local microenvironment. *Cell* 159(6):1312–1326.
34. Bruttger J, et al. (2015) Genetic cell ablation reveals clusters of local self-renewing microglia in the mammalian central nervous system. *Immunity* 43(1):92–106.
35. Suzuki R, Shimodaira H (2014) pvclust: Hierarchial clustering with P-values via multiscale bootstrap resampling. Available at cran.r-project.org/web/packages/pvclust/index.html. Accessed May 22, 2015.
36. Tremblay ME, et al. (2011) The role of microglia in the healthy brain. *J Neurosci* 31(45):16064–16069.
37. Gehrmann J, Banati RB (1995) Microglial turnover in the injured CNS: Activated microglia undergo delayed DNA fragmentation following peripheral nerve injury. *J Neuropathol Exp Neurol* 54(5):680–688.
38. Echeverry S, Shi XQ, Zhang J (2008) Characterization of cell proliferation in rat spinal cord following peripheral nerve injury and the relationship with neuropathic pain. *Pain* 135(1-2):37–47.
39. Huang Y, et al. (2009) Peripheral nerve lesion induces an up-regulation of Spy1 in rat spinal cord. *Cell Mol Neurobiol* 29(3):403–411.
40. Daneman R, Zhou L, Kebede AA, Barres BA (2010) Pericytes are required for blood-brain barrier integrity during embryogenesis. *Nature* 468(7323):562–566.
41. Lindahl P, Johansson BR, Levéen P, Betsholtz C (1997) Pericyte loss and microaneurysm formation in PDGF-B-deficient mice. *Science* 277(5323):242–245.
42. Fruttiger M, et al. (1999) Defective oligodendrocyte development and severe hypomyelination in PDGF-A knockout mice. *Development* 126(3):457–467.
43. Kucukdereli H, et al. (2011) Control of excitatory CNS synaptogenesis by astrocyte-secreted proteins Hevin and SPARC. *Proc Natl Acad Sci USA* 108(32):E440–E449.
44. Wilson JM, Young AB, Young AB, Kelley WN (1983) Hypoxanthine-guanine phosphoribosyltransferase deficiency. The molecular basis of the clinical syndromes. *N Engl J Med* 309(15):900–910.
45. Tunbridge EM, Harrison PJ, Weinberger DR (2006) Catechol-o-methyltransferase, cognition, and psychosis: Val158Met and beyond. *Biol Psychiatry* 60(2):141–151.
46. Guerreiro R, et al.; Alzheimer Genetic Analysis Group (2013) TREM2 variants in Alzheimer's disease. *N Engl J Med* 368(2):117–127.
47. Wang Y, et al. (2015) TREM2 lipid sensing sustains the microglial response in an Alzheimer's disease model. *Cell* 160(6):1061–1071.
48. Schafer DP, et al. (2012) Microglia sculpt postnatal neural circuits in an activity and complement-dependent manner. *Neuron* 74(4):691–705.
49. Chung, et al. (2013) Astrocytes mediate synapse elimination through MEGF10 and MERTK pathways. *Nature* 504(7480):394–400.
50. Rowley JW, et al. (2011) Genome-wide RNA-seq analysis of human and mouse platelet transcriptomes. *Blood* 118(14):e101–e111.
51. Sonnenberg A, Modderman PW, Hogervorst F (1988) Laminin receptor on platelets is the integrin VLA-6. *Nature* 336(6198):487–489.
52. Langenbach R, et al. (1995) Prostaglandin synthase 1 gene disruption in mice reduces arachidonic acid-induced inflammation and indomethacin-induced gastric ulceration. *Cell* 83(3):483–492.
53. Funk CD, Funk LB, Kennedy ME, Pong AS, Fitzgerald GA (1991) Human platelet/erythroleukemia cell prostaglandin G/H synthase: cDNA cloning, expression, and gene chromosomal assignment. *FASEB J* 5(9):2304–2312.
54. Nimmerjahn A, Kirchhoff F, Helmchen F (2005) Resting microglial cells are highly dynamic surveillants of brain parenchyma in vivo. *Science* 308(5726):1314–1318.
55. Davalos D, et al. (2005) ATP mediates rapid microglial response to local brain injury in vivo. *Nat Neurosci* 8(6):752–758.
56. Haynes SE, et al. (2006) The P2Y12 receptor regulates microglial activation by extracellular nucleotides. *Nat Neurosci* 9(12):1512–1519.
57. Lou N, et al. (2016) Purinergic receptor P2RY12-dependent microglial closure of the injured blood-brain barrier. *Proc Natl Acad Sci USA* 113(4):1074–1079.
58. Bardou P, Mariette J, Escudié F, Djemiel C, Klopp C (2014) jvenn: An interactive Venn diagram viewer. *BMC Bioinformatics* 15:293.